PETROLEUM EXPLORATION AND DEVELOPMENT
Volume 48, Issue 1, February 2021
Online English edition of the Chinese language journal

Available online at www.sciencedirect.com
ScienceDirect

Cite this article as: PETROL. EXPLOR. DEVELOP., 2021, 48(1): 136–145.

RESEARCH PAPER

Physical modeling of salt structures in the middle south Atlantic marginal basins and their controlling factors

YU Yixin[1, 2, *], TAO Chongzhi[3], SHI Shuaiyu[1, 2], YIN Jinyin[3], WU Changwu[3], LIU Jingjing[3]

1. State Key Laboratory of Petroleum Resources and Prospecting, China University of Petroleum, Beijing 102249, China;
2. Basin and Reservoir Research Center, China University of Petroleum, Beijing 102249, China;
3. Research Institute of Petroleum Exploration and Development, Sinopec, Beijing 100083, China

Abstract: With many types of salt structures developed in the Lower Cretaceous Aptian Formation, the passive continental marginal basins in the middle segment of the south Atlantic are hot areas of deep-water petroleum exploration. Based on analysis of differential deformations of salt structures, the influences of the inclination of subsalt slope, subsalt topographic reliefs and basement uplifting on the formation of salt structures were analyzed by physical modeling in this work. The experimental results show that the subsalt slopes in the middle West Africa basins are steeper, so the salt rock is likely to rapidly flow towards the ocean to form larger and fewer salt diapirs. In the Santos and Campos basins, the basement uplifts outside the basins are far from the provenances, which is conducive to the intrusion and accumulation of salt rock on the top of the basement uplifts. In contrast, in the middle West Africa, the basement uplifts are close to the basin margin, the residual salt layers above them are thin, and small triangular salt structures develop on both sides of the uplifts. Moreover, the uplifting of the African plate is also conducive to the full development of salt diapirs in the middle West Africa and results in large-scale thrust faults and folds in the front compressional zone.

Key words: South Atlantic; passive continental margin; Lower Cretacous; salt structure; subsalt framework; physical modeling

Introduction

Salt structure is a common structural style in petroliferous basins, and is closely related to hydrocarbon accumulation, as it has significant impact on trap formation, reservoir properties, source rock evolution, and hydrocarbon migration[1–9]. With special mechanical properties such as low density and weak compressional strength, salt rock has some unique deformation characteristics, and can form complex and variable structural styles, such as salt roller, salt pillow, salt diapir, salt tongue, salt sheet, salt wall, salt raft, salt weld, and salt-withdrawal minibasin[4,5,7,10–13]. The passive continental marginal basin in the middle segment of the south Atlantic is a typical area with well-developed salt structures[14–18], and also a hot area of deep-water petroleum exploration in the world[19–22]. The previous studies on the passive continental marginal basins in the middle segment of the south Atlantic were mainly focused on deformation styles, formation processes, and dynamic mechanisms of salt structures[14–18,23–28]. These studies paid more attention to deformation features of the salt layer and overlying formations. Recently, several papers reported the effects of base-salt relief on salt flow and suprasalt deformation patterns[27–28]. In addition, these studies mostly focused on a single basin or some key locations, and few compared and analyzed the basins on the both sides of the south Atlantic as a whole, hindering the deep understanding on development and dynamic mechanisms of salt structures in passive continental marginal basins. In this work, deformation of salt structures in the passive continental marginal basins on the both sides of the middle segment of the south Atlantic are compared and analyzed. The influences of subsalt slope, subsalt topographic relief and basement uplifting on the formation and evolution of salt structures are investigated by physical modeling.

1. Regional geological background

The middle segment of the south Atlantic refers to the

Received date: 29 Jun. 2020; **Revised date:** 06 Jan. 2021.
*** Corresponding author.** E-mail: yuxin0707@163.com
Foundation item: Supported by the China National Science and Technology Major Project (2016ZX05033, 2016ZX05026-007); National Natural Science Foundation of China (42072149).
https://doi.org/10.1016/S1876-3804(21)60010-1

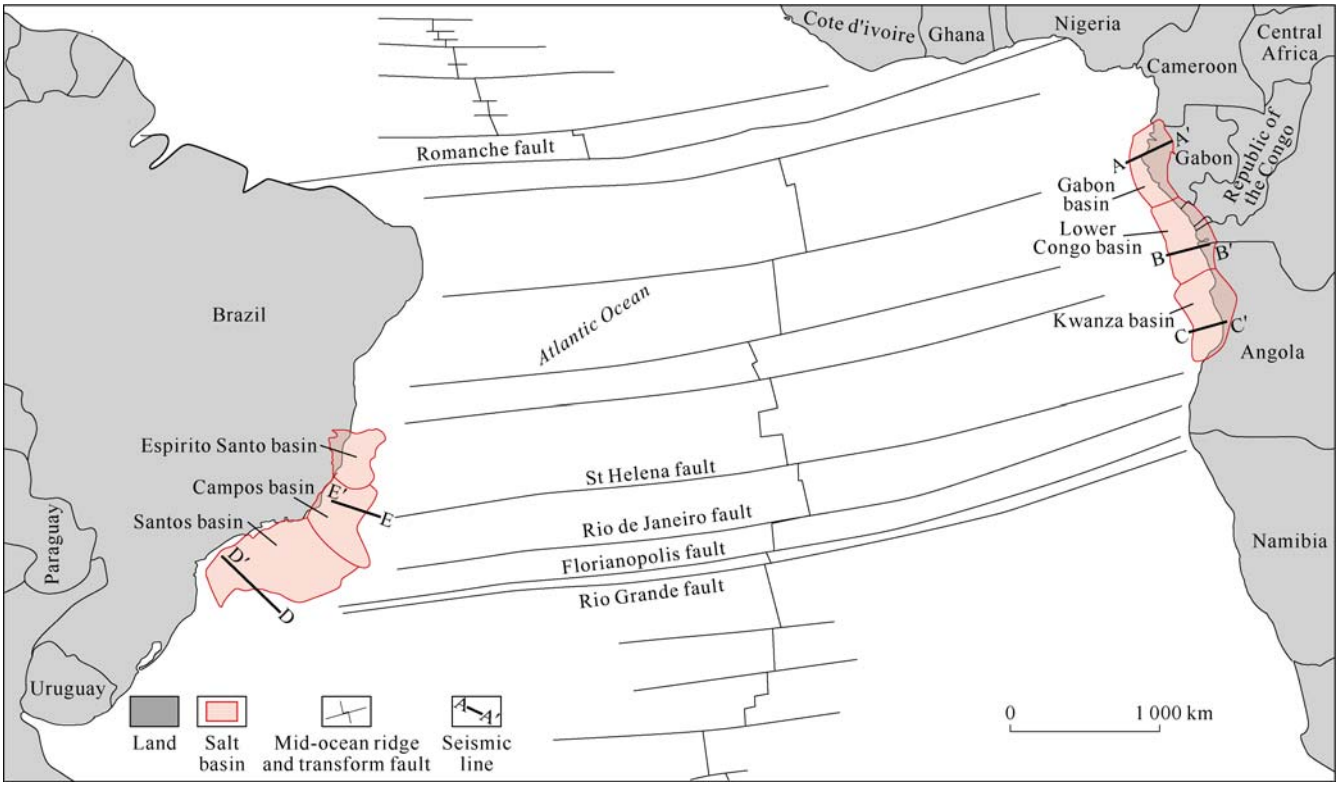

Fig. 1. Regional geological map of the passive continental marginal basins in the middle segment of the south Atlantic.

vast region located between the NEE-trending Florianopolis fault and Romanche fault[29]. Salt-bearing basins in this area include the Kwanza basin, the Lower Congo basin and the Gabon basin in West Africa continental margin, and the Santos basin, the Campos basin, and the Espirito Santo basin in eastern Brazil (Fig. 1). The passive continental marginal basins on the both sides of the south Atlantic were formed due to sea-floor spreading under the influence of regional extension when the Laurasia and Gondwana continents broke up after the Late Triassic. The basins have mainly experienced pre-rifting, rifting, transition and drifting stages[22,30–32] (Fig. 2). Corresponding to the four evolution stages, the basins have four mega-sedimentary sequences, namely the pre-rifting sequence, rifting continental sequence, transition salt-bearing sequence and drifting sequence (Fig. 2).

The transition stage during the late Aptian of Early Cretaceous is the initial formation stage of the passive continental margins of the south Atlantic. During this period, the basins were dominated by thermal subsidence, and the intensive tectonic movement basically ceased, and only some local and isolated fault blocks had adjustment. Due to the obstruction of the Walvis ridge, the basins in the middle segment of the south Atlantic were in semi-closed shallow water sedimentary environment. In the geological background of relatively stable tectonic subsidence, warm and dry climate and strong evaporation, a set of regionally distributed salt rock with a maximum thickness of 1 km deposited above the terrestrial and marine-terrestrial transitional strata[33]. During the stage of passive continental margin, the salt rock in the Lower Cretaceous Aptian flowed towards the ocean plastically, and thinned or thickened in some local areas, forming many types of salt structures in the basins. These salt structures influenced oil and gas accumulation from the aspects of trap development, reservoir properties, and hydrocarbon migration[9,17–20,31].

2. Deformation of salt structures

Controlled by the salt rock in the Lower Cretaceous Aptian, the structural deformation of the passive continental marginal basins in the middle segment of the south Atlantic exhibits obvious structural zonation from the continent to the ocean[7,15–18]. The salt-bearing basins in the middle West Africa can be divided into back extensional zone, central transition zone, and front compressional zone (Fig. 3). The deep-water basins in Brazil can be divided into nearshore low concave zone, middle low uplift zone, offshore low concave zone, and outer basement plateau zone from the land to the ocean (Fig. 4). Influenced by base-salt relief, overburden progradation rate and regional geological background etc, salt deformations in the passive continental marginal basins in the middle segment of the south Atlantic have some different characteristics.

2.1. Salt structures in the middle West Africa basins

The subsalt basement of the passive continental marginal basins in the middle West Africa is a westward inclined slope with many west-dipping normal faults. Near

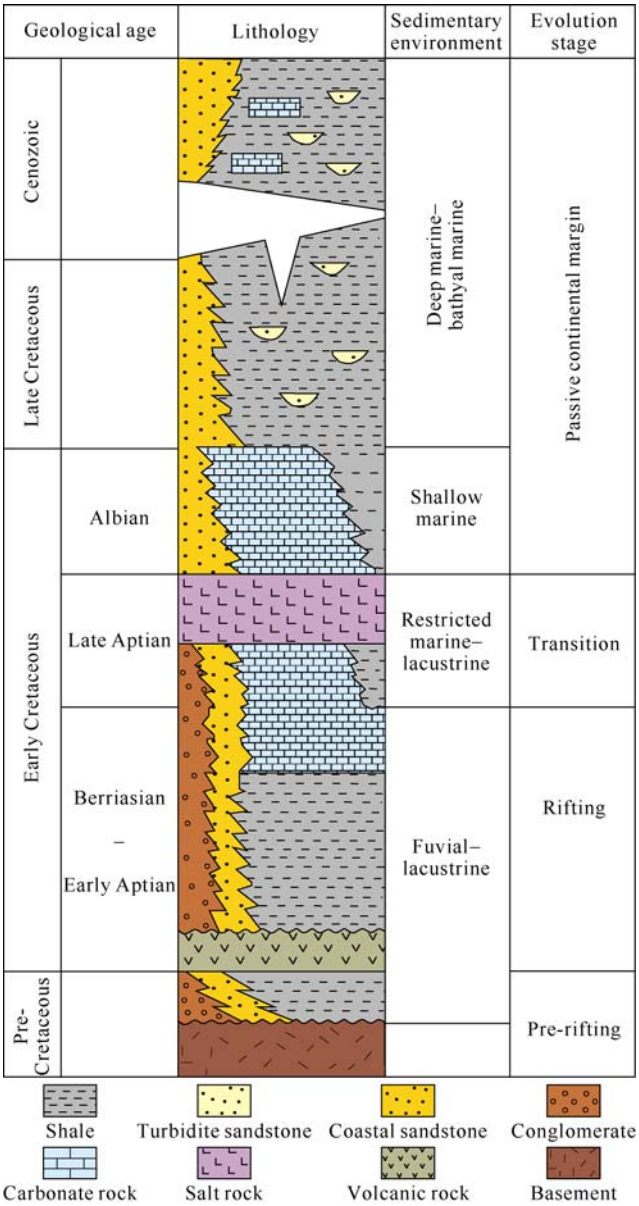

Fig. 2. Comprehensive stratigraphic column of the passive continental marginal basins in the middle segment of the south Atlantic (modified from Reference [22]).

the land side, are thick Lower Cretaceous and a basement uplift (or the Atlantic hinge zone). The stratum on the basement uplift top has been seriously eroded (Fig. 3). In the back extensional zone, the salt layer is generally thin, and is absent in some local areas. There are mainly normal faults, salt rollers, salt welds, and raft structures in this zone (Fig. 3). The normal faults are mostly inclined toward the ocean, detach on the top salt layer, and have some small triangle salt rollers in the footwall. According to formation ages, the raft structures can be further divided into the Cretaceous and Neogene raft structures. The Cretaceous raft structures mainly turned up near the land side, where a series of listric faults were formed during the salt detachement movement. The listric faults detached in the salt layer and ended upward in the Cretaceous (Fig. 3b). There are listric normal faults seaward in the Neogene. The strata on two sides of the listric faults have obvious differential sliding, and the synsedimentary strata on the hangingwall have rolling anticlines, resulting in the formation of raft structures in the Neogene (Fig. 3b).

The central transitional zone is located in the foot of the continental slope, where there are salt diapirs with eminent piercing feature and salt-withdrawal sags between salt diapirs (Fig. 3). On the whole, in this zone, faults are fewer, salt diapirs near the land are larger than salt rollers and have two wings quite symmetrical, and in conformable contact with the overlying formation in local areas. Towards the ocean, the salt diapirs are higher. For example, the salt diapirs in the Kwanza basin and Gabon basin have maximum uplifting height of about 4 km, and some are close to the seabed (Fig. 3a, c). The salt rock in some areas was squeezed into the Neogene seaward, thus forming salt tongues (Fig. 3c). If the intrusion is serious enough, isolated salt tongues would be formed (Fig. 3a). The front compressional zone is located near the deep ocean side of the basins, where the salt rock from the continent accumulates and thickens, reaching up 3 km thick (Fig. 3c). Influenced by compressional stress, thrust faults are common in this zone, and the salt rock squeezes and thrusts along the faults sometimes, leading to folds of the overlying stratum (Fig. 3b).

2.2. Salt structures in the Brazil deepwater area

The salt base in the Santos basin has an obvious shape of slope near the land, toward the ocean, the slope gradually flattens, and a rift system turns up (Fig. 4a). Different from the salt basins in the middle West Africa, the Santos basin has an outer basement plateau (the Sao Paulo plateau) on the deep ocean side, where thick Aptian salt rock deposit (Fig. 4a). In the Campos basin, the bottom of the salt layer has a shape of slope inclining toward the ocean on the whole. The subsalt basement has Badejo uplift, central uplift, and outer highland, showing the frame of 3 uplifts alternate with two sags, but the outer highland is significantly narrower than that of the Santos basin (Fig. 4b).

In the Santos basin and Campos basin, there develop normal faults dipping toward the land, salt rollers, and salt welds in the nearshore parts (Fig. 4); normal faults dipping toward the ocean and salt rollers in the footwalls of the normal faults in the part near the ocean. The central regions of the two basins (mainly the central low uplift zone) have the characteristics of bilateral extension, with faults inclining toward the land and the ocean. In the outer basement plateau zone and the nearshore low concave zone of the Santos basin and Campos basin, the salt layers are in thick layer (in general more than 1 km), with salt diapirs in some local parts (Fig. 4). Compared with the salt-bearing basins in the middle West Africa, the Santos and Campos basins have thicker salt layers above the outer basement plateau, but not so prominent

piercing salt diapirs (Figs. 3 and 4).

3. Physical modeling

3.1. Experimental materials

According to the similarity principle and modeling materials used commonly in previous studies[24,27,35–38], we used ductile silicone to simulate salt rock with Newtonian fluid characteristics, and dry and loose pure quartz sand to simulate the overlying sedimentary rock. The subsalt slope and uplift were simulated by steel plate and hard rubber block.

Under ambient temperature, the silicone had a density of 987 kg/m^3, with near-Newtonian characteristics. The silicone had a dynamic viscosity of 5×10^4 Pa·s at the strain rate less than 3×10^{-3} s^{-1}, which is close to the rheological features of salt rock. The quartz sand had a grain size of 100–400 μm, a bulk density of 1500 kg·m^{-3}, and a cohesive force of 200 Pa. In the natural gravity field, the deformation of the quartz sand satisfies the Mohr-Coulomb failure criterion, which is close to the brittle deformation

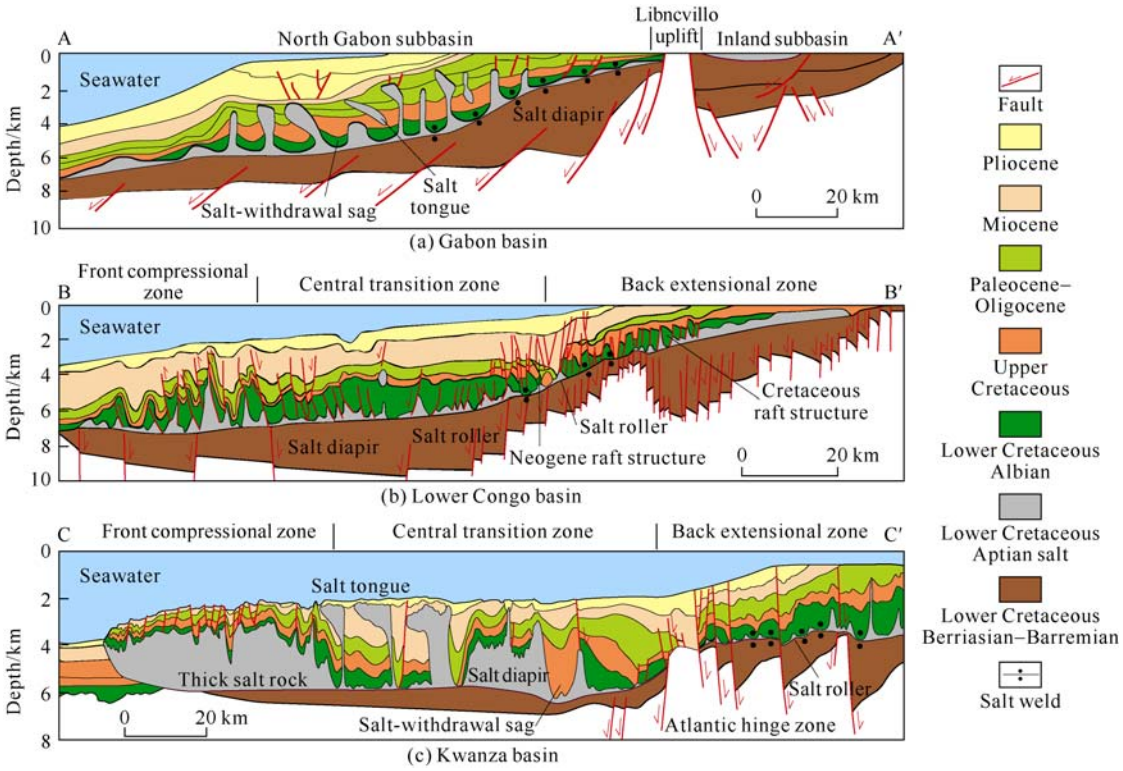

Fig. 3. Regional geological sections of the salt-bearing basins in the middle West Africa (modified from Reference [34]; see Fig. 1 for the section locations).

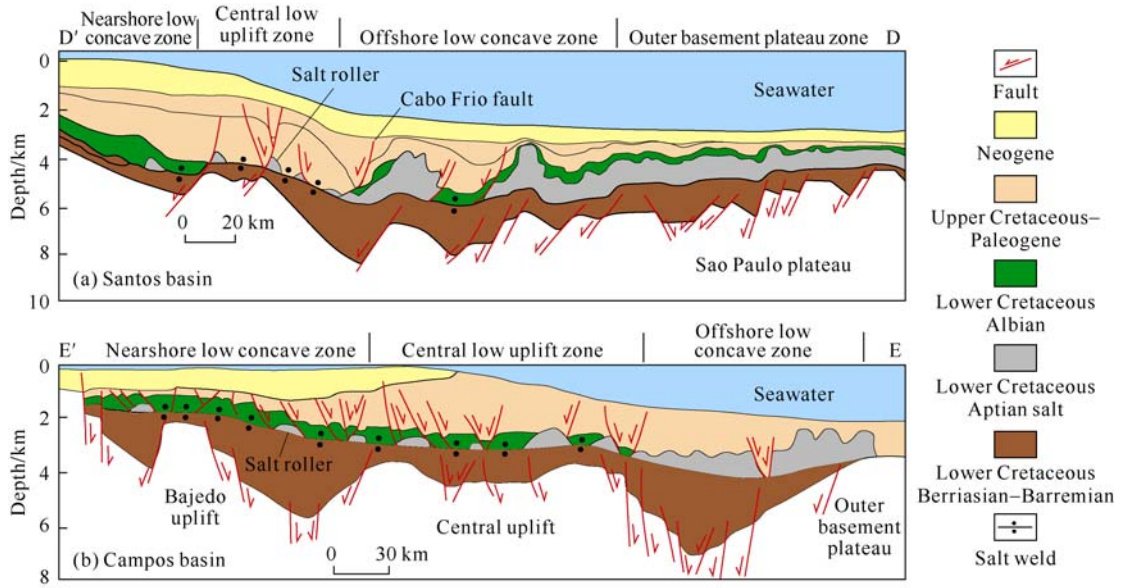

Fig. 4. Regional geological sections of the salt-bearing basins in Brazil deepwater (modified from Reference [34]; see Fig. 1 for the section locations).

Table 1. Experiment parameters of the physical model of salt structures in the middle segment of the south Atlantic.

Model	Gravity acceleration/(m·s^{-2})	Length/m	Density/(kg·m^{-3})		Viscosity/(Pa·s)	Time/h
Geological model	9.8	2×10^{5}	2 700 (Overlying stratum)	2 200 (Salt)	1×10^{17} (Salt)	9.5×10^{11}
Physical model	9.8	0.8	1 500 (Quartz sand)	987 (Silicone)	5×10^{4} (Silicone)	12–120
Scaled coefficient	1.0	4×10^{-6}	0.55	0.45	5×10^{-13}	$(0.12–1.20)\times10^{-10}$

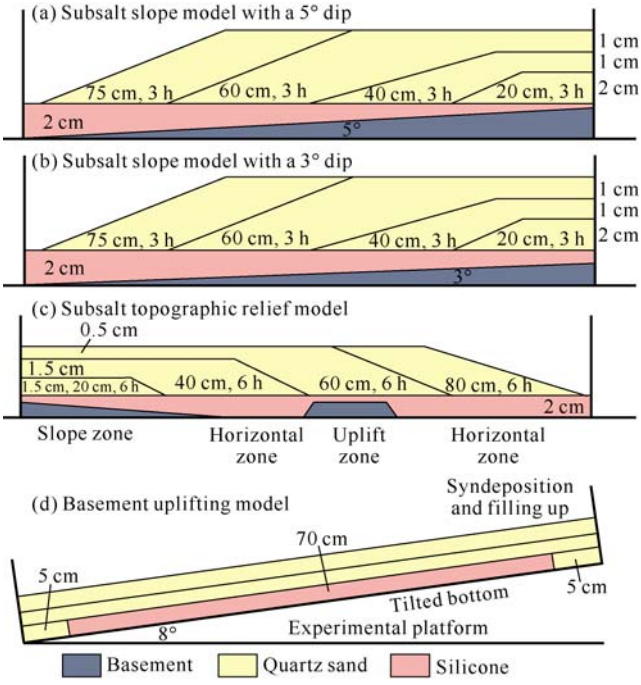

Fig. 5. Schematic diagrams showing the physical model setup.

behavior of sedimentary rock in the shallow crust[39]. In this study, in order to clearly observe the processes and characteristics of deformation, some quartz sand layers were colored as the marker layers. Table 1 shows the parameters and their scaled coefficients of the actual geological model and physical model, which basically meet the similarity principle of scaled physical modeling.

3.2. Model design

Based on the geological background and deformation characteristics of salt structures in the passive continental marginal basins in the middle segment of the south Atlantic (Figs. 3 and 4), we designed four physical models to find out the effects of subsalt slope, subsalt topographic relief and plate uplifting on the formation of salt structures (Fig. 5).

In order to analyze the influence of subsalt slope on the development of salt structure, two models were designed in this study. The two models were both 80×20 cm in size, with two fixed lateral plates. A PVC plate 80 cm long was used to simulate the basement slope. According to the previous study results[24,40], the dips of the subsalt slope were set at 5° and 3°, respectively, to simulate the passive continental marginal slopes with different tilting degrees in the middle segment of the south Atlantic (Fig. 5a, 5b). Firstly, a silicone layer about 2 cm thick was laid above the slope, and then the model was set aside for about 10 h to wait for the top silicone layer to turn horizontal and expel gas bubbles. Subsequently, a quartz sand layer 20 cm long was added in the left side of the model every 3 h, simulating the sediment aggradation in the continental margin.

Although the subsalt basements of the middle West Africa and the deepwater Brazilian show obvious uplift and depression structure, they have big differences in uplift and depression shapes and uplift locations. The basement uplifts of the salt-bearing basins in the middle West Africa (e.g. the Libncvillo uplift and the Atlantic hinge belt) are close to the land (Fig. 3), while the basement uplifts of the deepwater basins in Brazil (e.g. the Sao Paulo plateau) are close to the ocean (Fig. 4). Previous physical modeling has confirmed that the salt above the basement uplift near the provenance is relatively thin, and some small triangular salt diapirs are formed on both sides of the basement uplift[38]. To compare the influences of subsalt basement uplifts at different locations on the development of salt structures, we designed a model shown in Fig. 5c. The model was 80×20 cm, with two fixed lateral sides. The basement included a slope zone, a horizontal zone, and an uplift zone to simulate the continental slope, subsalt depression zone and subsalt uplift zone, respectively. The uplift belt was closer to the right side of the model far from the provenance (Fig. 5c). A silicone layer about 2 cm thick was laid above the basement, and the model was set aside quietly for about 10 h, to wait for the top silicone layer becoming horizontal and expelling gas bubbles. Then, a quartz sand layer 10 cm long was laid in the right side of the model every 3 h.

Regional studies indicated that the African plate had been uplifted during the Cenozoic, which might have some impact on salt structural deformation in the salt-bearing basins of the West Africa[41–42]. For this, we designed a model shown in Fig. 5d. The model had a piece of smooth glass 80 cm long as base, a 70 cm-long silicone layer above the glass, and 5cm-long quartz sand layers on the left and right sides of the silicone layer to simulate the blocking of the overlying sediments to the salt layer (Fig. 3). The base of the model was initially horizontal, and the right side of the model would be gradually tilted to a maximum slope of 8° during the modeling process (to make the experimental results more obvious, the tilting angle was larger than the actual degree). At the beginning of the modeling, a quartz sand layer was laid above the silicone layer. With the flow of

the early quartz sand layer during the experiment process, quartz sand was added to fill every 12 hours to level up the model. The total duration of the modeling was 120 h.

As there was cohesion between the silicone and the lateral glass plate, which would influence the modeling results, the models were fixed by filling sand and watering on the surface after the experiments were finished. Then the models were cut along the long axis direction to better observe the internal deformation characteristics of the silicone and quartz sand layer.

4. Results and discussion

4.1. Subsalt slope models

In the model with a subsalt slope dip of 5°, the silicone began to flow down the slope after about 3.5 h. At this time, the overall characteristics of silicone flow were not very significant, and the overlying sand layer on the left side of the model had only two normal faults (Fig. 6a). As the sand layer gradually progradated toward to the slope toe, under the influence of gravity sliding and differential loading of the overburden, the silicone flowed more obviously down slope, and several large faults turned up in the overlying sand layer (Fig. 6b). In the model with a subsalt slope dip of 3°, the flow characteristics of the silicone were roughly similar to the above model, but the overlying sand layer had more faults. At last, the models were cut. In the internal section of the subsalt slope model with a dip of 5°, there were six large scale listric normal faults and several small normal faults in the overlying sand layer, and the layers cut by the faults gradually became new towards the slope toe (Fig. 6c, 6d). In addition, in the right section of the model, three salt rollers were

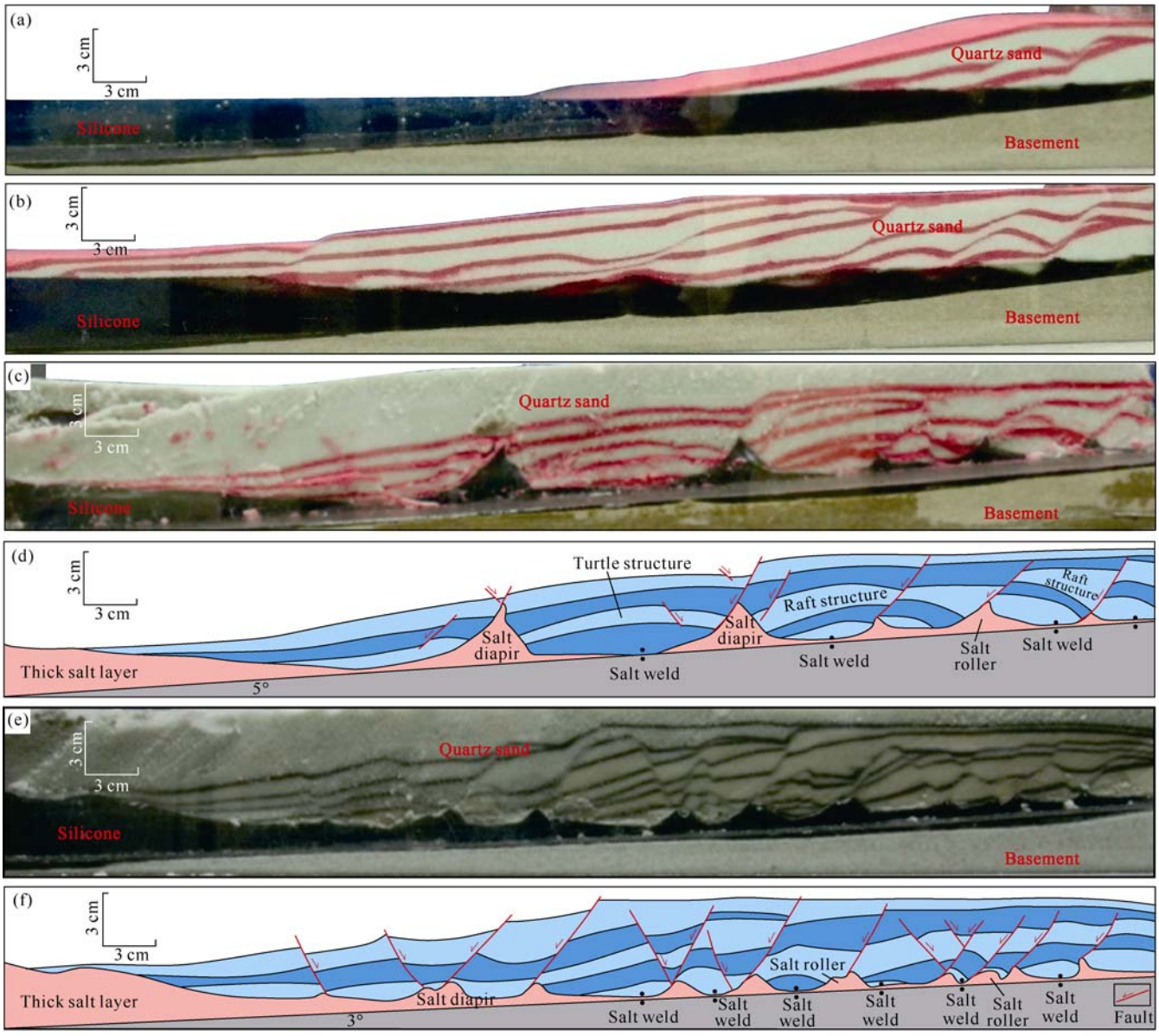

Fig. 6. Modeling processes and results of the subsalt slope models with different dips. (a) and (b) are the photos 3.5 h and 7 h into modeling of the subsalt slope model with a dip of 5°; (c) and (d) are the photos and interpretations of the subsalt slope model with a dip of 5°; (e) and (f) are the photos and interpretations of the subsalt slope model with a dip of 3°.

formed in the footwalls of normal faults, and raft structures were also formed in the sand layer in the hanging walls of the normal faults. Moreover, the sand layers of raft structures gradually became new towards the slope toe due to fault activity. This is similar to the Cretaceous raft structure on the land side and the Neogene raft structure on the seaside of the salt-bearing basins in the middle West Africa (Fig. 3b). In the middle section of the slope, there were two large-scale salt diapirs, and the sand layers at the top of the diapirs collapsed, forming normal faults and small grabens. Influenced by salt withdrawal activity, turtle structures developed between the two salt diapirs, and the salt welding areas were also relatively large (Fig. 6d). In the subsalt slope model with a dip of 3°, the overall deformation characteristics were similar to those of the model with the subsalt slope of 5°, but this model had more and larger normal faults in the overlying sand layers, and the grabens at the top of salt diapirs were also larger. In addition, this model had salt rollers, diapirs and salt welds larger in number but much smaller in scale than the former model (Fig. 6e, 6f).

The modeling results of the two comparative models show that the steeper subsalt slope facilitates rapid flow of salt toward the ocean due to gravity sliding and differential loading. As a result, salt structures develop rapidly, and are larger in scale and smaller in number. The salt welding areas between salt structures are also larger (Fig. 6e). The above modeling results are similar to the salt-bearing basins in the continental margin of the West Africa (Fig. 3). On the contrary, the gentler subsalt slope is conducive to slow flow of salt, salt structures can develop fully, but are smaller in scale; and a large number of normal faults can also develop in the overlying stratum (Fig. 6f), these are similar to the structural features of the salt basins in the deepwater Brazil (Fig. 4).

4.2. Subsalt topographic relief models

In the model with a subsalt uplift far from the provenance, 2.5 h into the modeling, the silicone above the upper slope began to flow, and a normal fault was also formed in the overlying sand layer at the slope top (Fig. 7a). As the sand layer gradually prograded toward to the right side of the model, the silicone flow and faulting in the overlying sand layer were more obvious. At the end of the experiment, several salt structures of different shapes were formed in the basement slope zone, the horizontal zone and the uplift zone (Fig. 7b). In the internal section of the model, it can be seen that several large-scale salt rollers and salt diapirs developed in the subsalt slope and horizontal zones. There were several normal faults on the top of the salt rollers and salt diapirs, which formed some small grabens. In the right section of the model, thicker silicone gathered, with the characteristics of extrusion and thrust in local parts (Fig. 7c). Besides, salt thickening occurred at the top of the basement uplift in the middle part of the model (Fig. 7c), suggesting that the top of the subsalt uplift far from the provenances is a weak area favorable for salt intrusion and accumulation[43–44]. The modeling results are significantly different from the salt thickness and deformation characteristics of the model with a basement uplift close to the provenance (Fig. 7c, d). It should be noted that the top surface of the thick

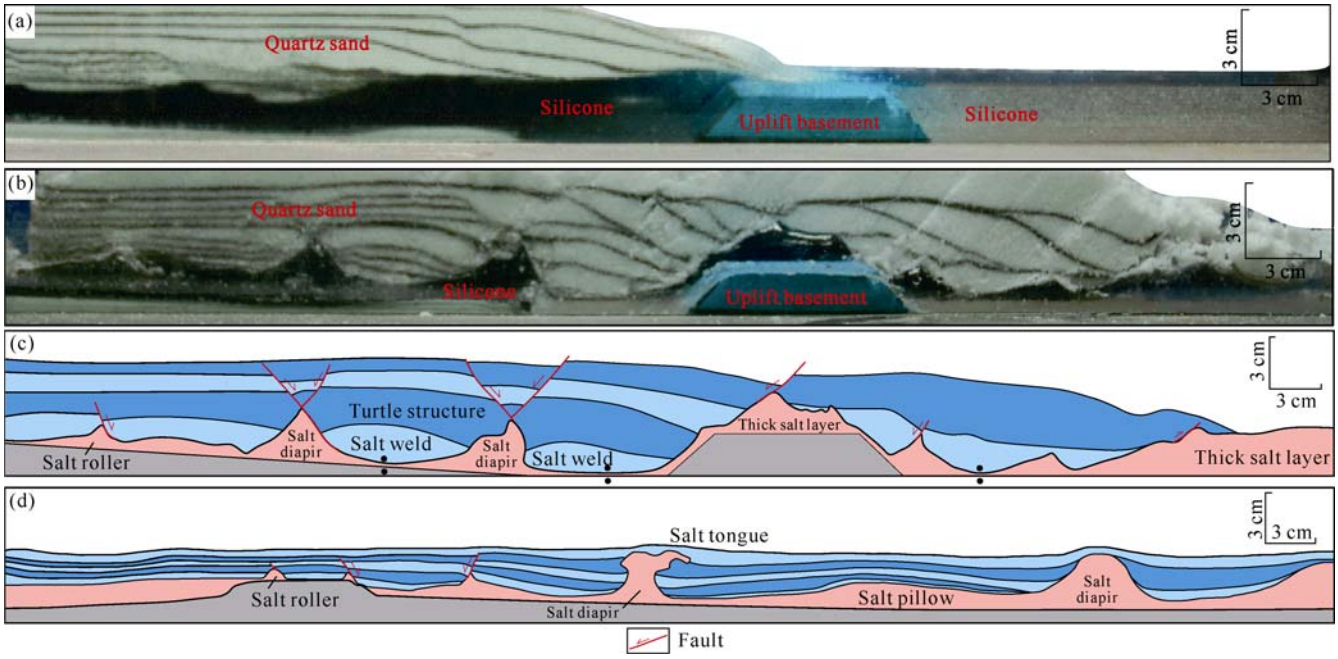

Fig. 7. Modeling processes and results of the subsalt topographic relief models. (a) The photo 2.5 h into modeling of the model with a subsalt uplift far from the provenance; (b) and (c) are the result photos and interpretations of the model with a subsalt uplift far from the provenance; and (d) the interpretation of the model with a subsalt uplift close to the provenance, which is modified from the Reference [38].

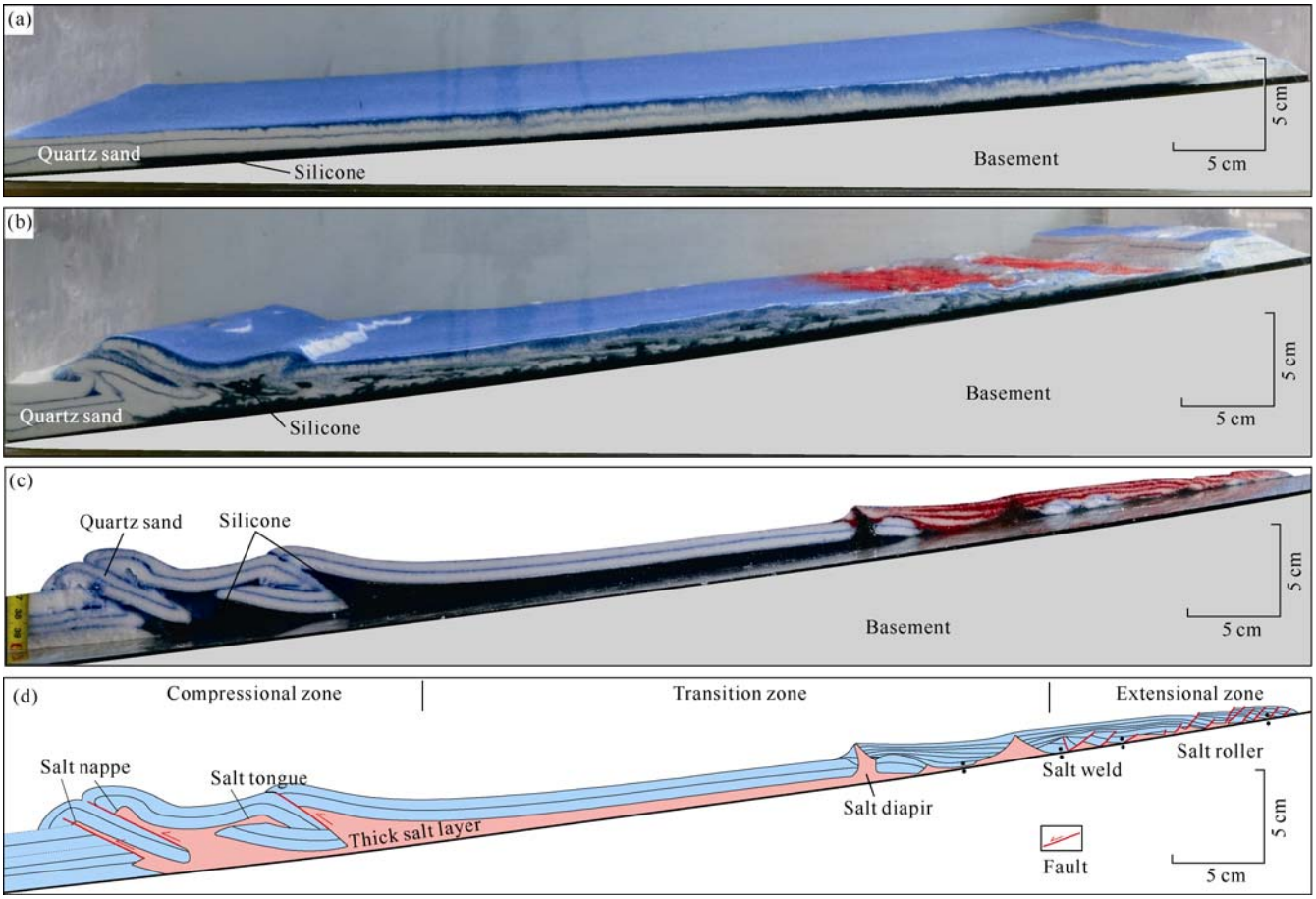

Fig. 8. Modeling process and results of the basement uplifting model. (a) The photo 12 h into modeling; (b) the photo 60 h into modeling; (c) and (d) the result photos and their interpretations 120 h into modeling.

salt layer above the basement uplift in the model was not a plane, but had local sags and faults (Fig. 7c), which is similar to the deformation characteristics of the salt above the Sao Paulo plateau in the Santos Basin (Fig. 4b). The thicker salt layers above the basement uplifts have strong impact on hydrocarbon accumulation in the subsalt carbonate reservoirs. For example, the main reservoir of the Tupi giant oilfield in BM-S-11 block of the Santos basin discovered in 2006 is the carbonate rock below the Aptian salt rock. The salt rock more than 2000 m thick can not only seal oil and gas in the subsalt carbonate reservoirs, but also facilitate the transfer of subsalt heat to the shallow layer, so the subsalt carbonate reservoirs can still keep a high proportion of initial porosity even under large burial depth[7].

4.3. Basement uplifting model

At the beginning of the modeling, the horizontal base of the model was tilted to the slope angle of 5°. After 12 h, the model had no obvious deformation, except slight extension and thrust at the positions where the quartz sand blocked silicone in the upper and lower slope (Fig. 8a). After 20 h, the base of the model was tilted to a slope angle of 8°. 60 h into the modeling, the model had significant extension and compression deformations in the right and left sides, respectively (Fig. 8b). Subsequently, the extension and thrust deformations strengthened further. At last, several normal faults appeared and the silicone thinned obviously in the right side of the model. In the left side of the model, several thrust faults and anticlines turned up, along which the silicone intruded and thrusted. In contrast, the silicone and the sand layer in the middle part of the model had only slight deformation (Fig. 8c). In the internal section of the cut model, the silicone and the sand layer gradually thickened from the extensional zone to the compressional zone, and the structural deformation features have obvious zonation (Fig. 8d). The extensional zone on the right side of the model was characterized by normal faults and small salt rollers. The central transitional zone had mainly large-scale salt diapirs of different shapes, and some salt diapirs had penetrated the overlying quartz sand layer and reached the model surface. The front compressional zone in the left side of the model was mainly characterized by thrust faults and thick salt bodies; in local parts, the salt body was obviously squeezed, resulting in the formation of salt nappes and isolated salt tongues, and folds in the overlying sand layer. These are very similar to the deformation characteristics of salt structures in the front compressional zone of the Lower Congo basin (Figs.

3b and 8d). The modeling results show that significant gravity sliding and spreading are likely to form thrust faults primarily and folds secondarily in the front compressional zone. The thinning of the overlying stratum from the compressional zone to the extensional zone also reflects the control of the basement tilting extent on structural style.

5. Conclusions

Many types of salt structures occur in the passive continental marginal basins in the middle segment of the south Atlantic, and show obvious structural zonation from the land to the sea. In the salt-bearing basins in the middle West Africa, the subsalt slopes have larger dips, which can make the salt flow rapidly towards the ocean, resulting in larger and fewer salt diapirs, and larger salt welding areas. In contrast, the subsalt slopes of the deepwater basins in Brazil are gentler, which is conducive to slow flow of salt. As a result, salt structures in the deepwater basins in Brazil can fully develop, but are smaller in scale generally. The uplifting of the African plate made it possible to form large-scale thrust faults and folds in the front compressional zone under the effect of gravity sliding. The outer basement uplifts of the Santos basin and Campos basin in Brazil are far from the provenances, and salt is likely to intrude and built up to large thickness at the top of the uplifts. On the contrary, the subsalt basement uplifts in the middle West Africa basins are close to the provenances, the salt above the basement uplifts is thin (or missing), and small-scale salt rollers come up on both sides of the basement uplifts.

References

[1] JACKSON M P A. Retrospective salt tectonics: JACKSON M P A, ROBERTS D G, SNELSON S. Salt tectonic: A global perspective. Tulsa: AAPG, 1995: 1–28.

[2] GE Hongxing, JACKSON M P A. Salt structures, hydrocarbon traps and mineral deposits. Journal of Nanjing University (Natural Science Edition), 1996, 32(4): 640–649.

[3] VOLOZH V, TALBOT C, ZADEH A I. Salt structures and hydrocarbons in the Pricaspian Basin. AAPG Bulletin, 2003, 87(2): 313–334.

[4] HUDEC M R, JACKSON M P A. Terra infirma: Understanding salt tectonics. Earth Science Reviews, 2007, 82(1/2): 1–28.

[5] WARREN J K. Evaporites through time: Tectonic, climatic and eustatic controls in marine and nonmarine deposits. Earth Science Reviews, 2010, 98(3/4): 217–268.

[6] YU Yixin, ZHOU Xinhuai, PENG Wenxu, et al. An overview on salt structures. Geotectonica et Metallogenia, 2011, 35(2): 169–182.

[7] JACKSON M P A, HUDEC M R. Salt tectonics: Principles and practice. Cambridge: Cambridge University Press, 2017.

[8] WANG Mingwen, LUO Gang, SUN Yunqiang, et al. Numerical modeling of stress perturbations caused by geometric changes of salt bodies. Petroleum Exploration and Development, 2020, 47(2): 309–320.

[9] ZHANG Gongcheng, QU Hongjun, ZHANG Fenglian, et al. Major new discoveries of oil and gas in global deep waters and enlightenment. Acta Petrolei Sinica, 2019, 40(1): 1–34.

[10] SENI S J, JACKSON M P A. Evolution of salt structures, east Texas diapir province, part 1: Sedimentary record of halokinesis. AAPG Bulletin, 1983, 67(8): 1219–1244.

[11] MCBRIDE B C, ROWAN M G, WEIMER P. The evolution of allochthonous salt systems, Western Green Canyon and Ewing Bank(offshore Louisiana), Northern Gulf of Mexico. AAPG Bulletin, 1998, 82(5): 1013–1036.

[12] ROWAN M G, JACKSON M P A, TRUDGILL B D. Salt-related fault families and fault welds in the Northern Gulf of Mexico. AAPG Bulletin, 1999, 83(9): 1454–1484.

[13] HUDEC M R, JACKSON M P A. The salt mine: A digital atlas of salt tectonics. Tulsa: AAPG, 2011.

[14] MEISLING K E, COBBOLD P R, MOUNT V S. Segmentation of an obliquely rifted margin, Campos and Santos Basins, southeastern Brazil. AAPG Bulletin, 2001, 85(11): 1903–1924.

[15] TARI G, MOLNAR J, ASHTON P. Examples of salt tectonics from West Africa: A comparative approach: ARTHUR T J, MACGREGOR D S, CAMERON N R. Petroleum geology of Africa: New themes and developing technologies. London: Geological Society, 2003: 85–104.

[16] HUDEC M R, JACKSON M P A. Regional restoration across the Kwanza Basin, Angola: Salt tectonics triggered by repeated uplift of a metastable passive margin. AAPG Bulletin, 2004, 88(7): 971–990.

[17] QUIRK D G, Salt tectonics on passive margins: Examples from Santos, Campos and Kwanza Basins: ALSOP G I, ARCHER S G, HARTLEY A J, et al. Salt tectonics, sediments and prospectivity. London: Geological Society, 2012: 207–244.

[18] MOHRIAKI W U, SZATMARI P, ANJOS S. Salt: Geology and tectonics of selected Brazilian basins in their global context: ALSOP G I, ARCHER S G, HARTLEY A J, et al. Salt tectonics, sediments and prospectivity. London: Geological Society, 2012: 131–158.

[19] LIU Zuodong, LI Jianghai. Tectonic evolution and petroleum geology characteristics of petroliferous salt basins area along passive continental margin, west Africa. Marine Origin Petroleum Geology, 2009, 14(3): 46–52.

[20] GUO Jianyu, HAO Hongwen, LI Xiaoping. Geologic characteristic of hydrocarbon in the passive continental marginal basins of South America. Geoscience, 2009, 23(5): 916–922.

[21] STARK P, SMITH L K. Giant oil and gas fields of the

2000s: A new century ushers in deeper water, unconventionals, and more gas: MERRILL R K, STERNBACH C A. Giant fields of the decade 2000–2010. Tulsa: AAPG, 2017: 15–28.

[22] LIU Jingjing, WU Changwu, DING Feng. Basin types and hydrocarbon distribution in salt basins in the South Atlantic. Petroleum Geology & Experiment, 2018, 40(3): 372–380.

[23] HUDEC M R, JACKSON M P A. Structural segmentation, inversion, and salt tectonics on a passive margin: Evolution of the Inner Kwanza Basin, Angola. GSA Bulletin, 2002, 114(10): 1222–1244.

[24] FORT X, BRUN J P, CHAUVEL F. Salt tectonics on the Angolan margin, synsedimentary deformation processes. AAPG Bulletin, 2004, 88(11): 1523–1544.

[25] FETTER M. The role of basement tectonic reactivation on the structural evolution of Campos Basin, offshore Brazil: Evidence from 3D seismic analysis and section restoration. Marine and Petroleum Geology, 2009, 26(6): 873–886.

[26] BRUN J P, FORT X. Salt tectonics at passive margins: Geology versus models. Marine and Petroleum Geology, 2011, 28: 1123–1145.

[27] DOOLEY T P, HUDEC M R, CARRUTHERS D, et al. The effects of base-salt relief on salt flow and suprasalt deformation patterns: Part 1: Flow across simple steps in the base of salt. Interpretation, 2018, 5(1): SD1–SD23.

[28] PICHEL L M, JACKSON C A L, PEEL F, et al. Base-salt relief controls salt-tectonic structural style, Sao Paulo Plateau, Santos Basin, Brazil. Basin Research, 2020, 32: 453–484.

[29] BENIEST A, KOPTEV A, BUROV E. Numerical models for continental breakup: Implications for the South Atlantic. Earth and Planetary Science Letters, 2017, 461: 176–189.

[30] MOHRIAK W U, HOBBS R, DEWEY J F. Basin-forming processes and the deep structure of the Campos Basin, offshore Brazil. Marine and Petroleum Geology, 1990, 7(2): 94–122.

[31] WU Changwu. Hydrocarbon enrichment characteristics and exploration potentials in salt basins of South Atlantic. Xinjiang Petroleum Geology, 2015, 36(1): 121–126.

[32] LI Minggang. Structural characteristics and trap development patterns of pre-salt rift system in Santos Basin. Fault-block Oil & Gas Oilfield, 2017, 24(5): 608–612.

[33] LENTINI M R, FRASER S I, SUMNER H S, et al. Geodynamics of the central South Atlantic conjugate margins: Implications for hydrocarbon potential. Petroleum Geoscience, 2010, 16: 217–229.

[34] ENERGY IHS. International petroleum exploration and production database. https://my.ihs.com/Energy/Products, 2019.

[35] VENDEVILLE B C, GE H X, JACKSON M P A. Scaled models of salt tectonics during basement-induced extension. Petroleum Geoscience, 1995, 1(2): 179–183.

[36] DOOLEY T P, JACKSON M P A, HUDEC M R. Initiation and growth of salt-based thrust belts on passive margins: Results from physical models. Basin Research, 2007, 19(1): 165–177.

[37] YU Yixin, TANG Liangjie, YANG Wenjing, et al. Thick-skinned contractional salt structures in Kuqa depression, northern Tarim basin: Constraints from physical experiments. Acta Geologica Sinica, 2008, 82(2): 327–333.

[38] WU Zhenyun, YIN Hongwei, WANG Xin, et al. The structural styles and formation mechanism of salt structures in the Southern Precaspian Basin: Insights from seismic data and analog modeling. Marine and Petroleum Geology, 2015, 62: 58–76.

[39] GE Hongxing, VENDEVILLE B C, JACKSON M P A. Physical models of thick-skinned contractional salt tectonics in a foreland fold-and-thrust belt. Geological Journal of China Universities, 2004, 10(1): 39–49.

[40] PEEL F J. The engines of gravity-driven movement on passive margins: Quantifying the relative contribution of spreading vs. gravity sliding mechanisms. Tectonophysics, 2014, 633: 126–142.

[41] SAHAGIAN D. Epeirogenic motions of Africa as inferred from Cretaceous shoreline deposits. Tectonics, 1988, 7: 125–138.

[42] GURIRAUD R, BOSWORTH W, THIERRY J, et al. Phanerozoic geological evolution of Northern and Central Africa: An overview. Journal of African Earth Sciences, 2005, 43(1/2/3): 83–143.

[43] KOYI H, PETERSEN K. Influence of basement faults on the development of salt structures in the Danish Basin. Marine and Petroleum Geology, 1993, 10(4): 82–93.

[44] YU Yixin, TANG Liangjie, LI Jingchang, et al. Influence of basement faults on the development of salt structures in the Kuqa foreland fold and thrust belt, northern Tarim Basin. Acta Geologica Sinica, 2006, 80(3): 330–336.